Available online at www.sciencedirect.com
SCIENCE DIRECT®
ELSEVIER
International Journal of Multiphase Flow 30 (2004) 551–563
International Journal of Multiphase Flow
www.elsevier.com/locate/ijmulflow

The flow pattern map of a two-phase non-Newtonian liquid–gas flow in the vertical pipe

Marek Dziubinski *, Henryk Fidos, Marek Sosno

Faculty of Process and Environmental Engineering, Technical University of Lodz, 93-005 Lodz, Wolczanska 213, Poland

Received 12 February 2003; received in revised form 18 April 2004

Abstract

A map for the determination of flow pattern for two-phase flow of gas and non-Newtonian liquid in the vertical pipe has been presented. Our own experimental data confirm applicability of such a map.
© 2004 Elsevier Ltd. All rights reserved.

Keywords: Multi-phase flow; Non-Newtonian liquid; Flow pattern

1. Introduction

One of the basic problems in multi-phase flow is a possibility to predict a priori the structure of a multi-phase mixture flow on the basis of known values of the apparent flow velocity and properties of particular phases and flow geometry (a pipe diameter and the angle of its inclination).

As one knows, in the case of the two-phase flow of Newtonian liquid–gas mixture in vertical pipes in the uprising mode, five basic flow structures are distinguished in general. They are shown in a diagram in Fig. 1. In the case of highly viscous liquids (higher than 100 mPa·s), flow structures represented in Fig. 2 are observed.

Detailed characteristics and measuring methodology for setting the flow pattern of a two-phase liquid–gas flow can be found elsewhere, among others in Nicklin and Davidson (1962), Hewitt and Roberts (1969a,b), Delhaye (1976), Govier and Aziz (1982), Ikeda et al. (1983), McQuillan et al. (1985), Lee and Kim (1986) and Ulbrich (1986).

* Corresponding author. Tel.: +42-631-3700; fax: +42-636-5663.

0301-9322/$ - see front matter © 2004 Elsevier Ltd. All rights reserved.
doi:10.1016/j.ijmultiphaseflow.2004.04.005

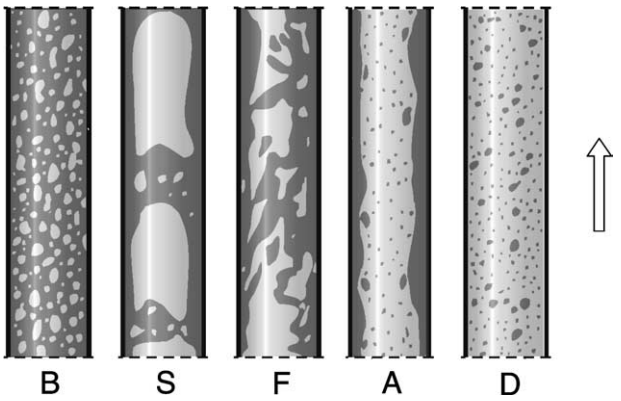

Fig. 1. Basic flow structures in vertical upward flow: B—bubble flow, S—slug flow, F—froth flow, A—annular flow, D—dispersed flow.

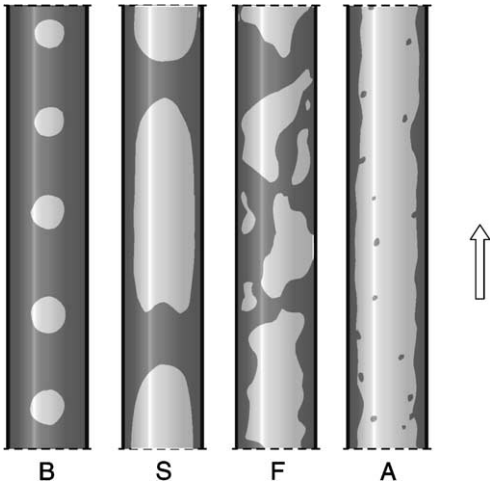

Fig. 2. Flow structures in highly viscous liquids: B—bubble flow, S—slug flow, F—froth flow, A—annular flow.

The ranges of particular flow structures are illustrated in diagrams called the flow maps. So far, dozens of such maps have been proposed in the available literature for the two-phase mixture of a Newtonian liquid and gas flowing in vertical pipes (Golan and Stenning, 1969–1970; Oshinowo and Charles, 1974; Taitel et al., 1980; Spedding and Ngyuen, 1980; Barnea et al., 1982; Crawford and Weisman, 1984; Spisak, 1986; Ulbrich (1989)). For instance, Spisak (1986) gives information on 32 maps for rising flow and 10 maps for down flow of the two-phase mixture. The most significant data are given in Table 1. On the basis of the analysis of flow maps presented in Table 1, it can be found that most of them have an experimental character. Only the map presented by Taitel et al. (1980) is based on a semi-theoretical model. It seems that the best description of experimental data is obtained using the maps proposed by Hewitt and Roberts (1969a,b), Taitel et al. (1980), Spisak (1986) and a universal map of Ulbrich (1989).

In the case of the two-phase flow of non-Newtonian liquids two maps representing flow of such mixture but only in horizontal pipes have been proposed (Chhabra and Richardson (1984),

Table 1
The review of the most significant flow pattern maps for two-phase Newtonian liquid–gas mixture flowing in vertical pipes

Authors (year)	Map coordinates	
	x	y
Govier et al., 1957	v_{SG}/v_{SL}	v_L
Griffith and Wallis, 1961	v_M	α_L
Hewitt and Roberts, 1969a,b	$V_{SL}^2 \cdot \rho_L$	$v_{SG}^2 \cdot \rho_G$
Golan and Stenning, 1969–1970	v_{SG}	v_{SL}
Oshinowo and Charles, 1974	$\frac{\mathrm{Fr}}{\left(\frac{\mu_L/\mu_{H_2O}}{\sqrt{\rho_L/\rho_{H_2O}\cdot(\sigma_L/\sigma_{H_2O})^3}}\right)}$	$\sqrt{\frac{v_{SG}}{v_{SL}}}$
Taitel et al., 1980	v_{SG}	v_{SL}
Spedding and Ngyuen, 1980	v_{SL}/v_{SG}	$\frac{v_L^2}{g\cdot d}$
Barnea et al., 1982	v_{SG}	v_{SL}
Spisak, 1986	$\frac{v_{SG}}{v_{SL}} \cdot \sqrt{\frac{\rho_G}{\rho_{air}} \cdot \frac{\rho_{H_2O}}{\rho_L}}$	$v_{SL} \cdot \sqrt{\frac{\rho_L}{\rho_{H_2O}}}$
Ulbrich, 1989	$\frac{v_{SG}}{v_{SL}} \cdot \sqrt{\frac{\rho_G}{\rho_{air}} \cdot \frac{\rho_{H_2O}}{\rho_L}}$	$v_{SL} \cdot \sqrt{\frac{\rho_L}{\rho_{H_2O}}}$

Dziubinski (1986)). On these maps a classical system of coordinates $v_{SL} = f(v_{SG})$ was used. In view of the increasing importance of the two-phase flows of non-Newtonian liquids, this problem requires intensive research.

The aim of this study was to develop a map of the rising flow of multi-phase mixtures of solid particles suspended in the non-Newtonian liquid and gas in vertical pipes.

2. Experimental set-up

Experiments were carried out in a set-up for testing multi-phase flow in vertical pipelines shown in Fig. 3 (Fidos, 2001). Non-Newtonian liquid solutions and suspensions of particles in non-Newtonian liquids were prepared in tank 1 and pumped by centrifugal pump 5 to a selected measuring Section 6. The medium flow rate was measured by Cole-Parmer (USA) and ENCO (Poland) electromagnetic flowmeters 7, 8.

Gas from the central pressure installation through a system of reducers and filters 14, 16 was supplied to the pipeline through a skew distributor 20—see Fig. 4. The gas flow rate was measured using a system of rotameters 17 and its pressure by means of manometer 19. The produced two-phase mixture flew through the flow-stabilising section to get to a selected measuring section.

Measuring sections consisted of glass pipes 50.5, 40.6 and 25.3 mm in diameter. The glass sections for flow structure observation were 2 m long (the total pipeline length was 5 m).

The type of multi-phase flow in vertical pipes was determined simultaneously by two methods: a visual observation (plus filming with a video camera) and recording of the readouts of opto-electronic sensors.

The optoelectronic sensors were located at a distance of 2, 3, 3.5 and 4 m from gas inlet to the measuring duct. The sensor structure is illustrated in Fig. 5. A concentrated light beam passed

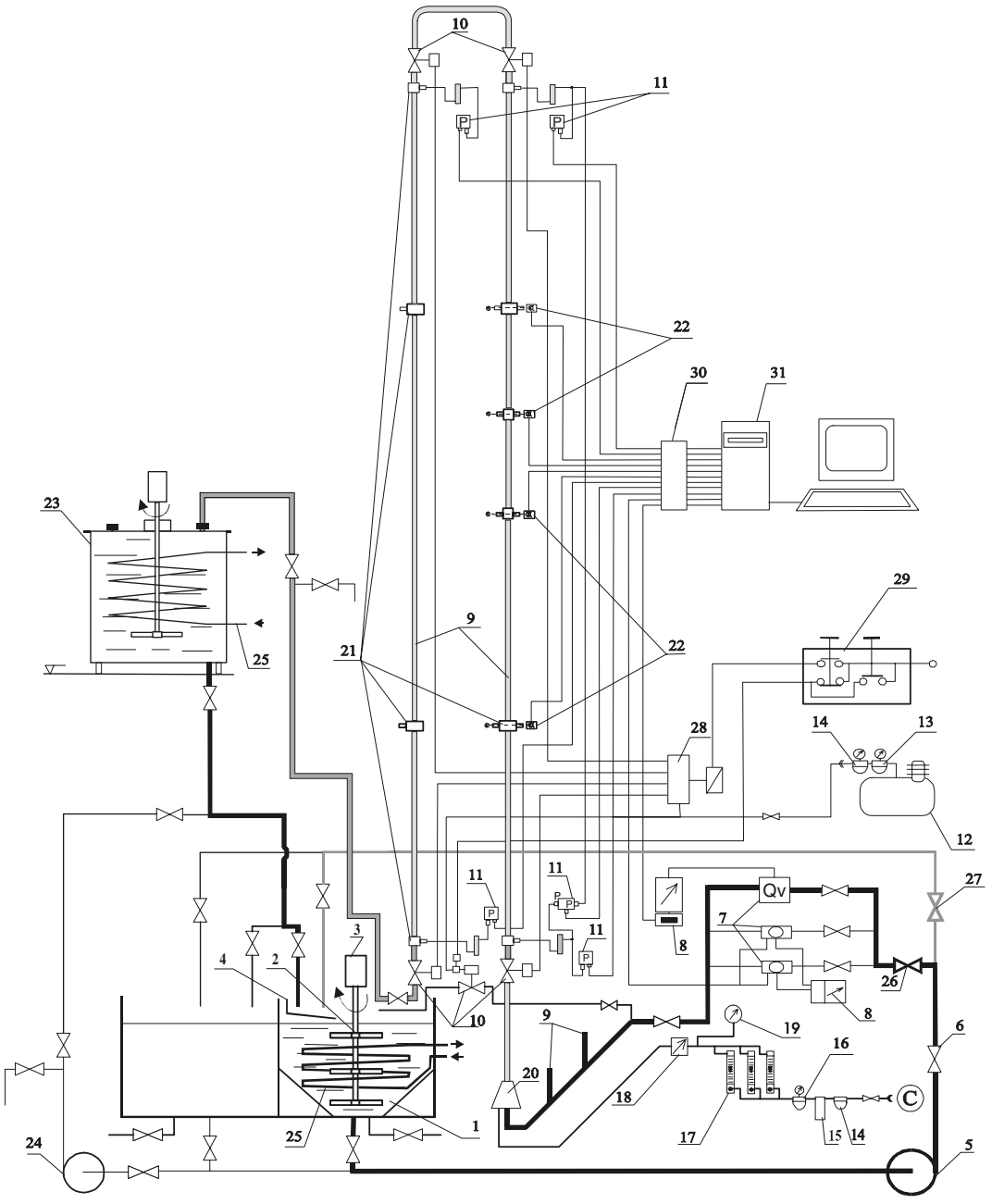

Fig. 3. Experimental set-up: 1—main tank, 2—blade impeller, 3—d.c. motor, 4—separation trough, 5—centrifugal pump to press slurry, 6—throttle, 7—electromagnetic flowmeter, 8—flowmeter converter, 9—glass measuring sections, 10—pneumatic valves, 11—pressure drop measuring sensors, 12—compressor, 13—pressure control, 14—oil trap, 15—air filter, 16—pressure control, 17—precision rotameters system, 18—electromagnetic valve, 19—manometer, 20—air distributor, 21—rings to install measuring sensors, 22—optoelectronic converters, 23—separation tank, 24—circulating pump, 25—coils, 26, 27—control valves, 28—pneumatic valve controller, 29—pneumatic valve switch key, 30—interface board, 31—computer with a data acquisition card.

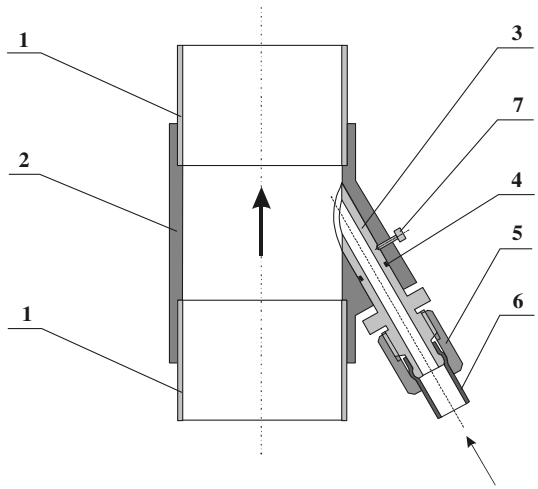

Fig. 4. Gas distributor: 1—metal pipe segments, 2—metal casing, 3—exchangeable nozzle, 4—rubber seal (o-ring), 5—packing nut, 6—gas pipe, 7—clamping screw.

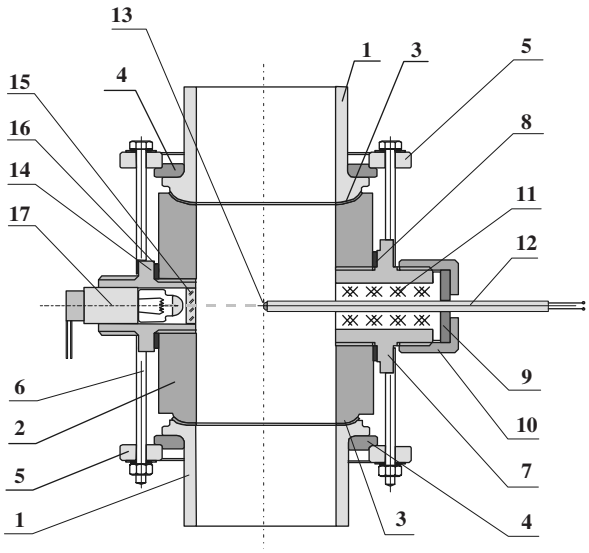

Fig. 5. Construction of optoelectronic sensor: 1—glass sections of the measuring pipeline, 2—ring to install measuring devices, 3—rubber gasket, 4—half-ring clamps, 5—flanges, 6—clamping screws, 7—longer connector pipe, 8—packing washer, 9—throttle, 10—screw cup, 11—teflon pad, 12—phototransistor holder (stainless steel pipe), 13—phototransistor BPYP 21, 14—shorter connector pipe, 15—polymethyl methacrylate window, 16—packing washer, 17—lamp holder.

through a flowing mixture to a phototransistor of a very small diameter (2 mm) located in a rigid thin metal tube in the pipe axis. After amplification, the signal from the phototransistor was

recorded in a computer data acquisition system. Very slight differences were observed in oscillograms recorded by subsequent optoelectronic sensors.

A basis for determination of the flow structure in the pipe were the readouts of two centrally placed optoelectronic sensors supported by filming and visual observation in the centre of the pipe section between the above mentioned sensors (the distance between them was 0.5 m).

Typical runs of "oscillograms" obtained by means of the optoelectronic sensors dependent on the flow structures are shown in Fig. 6. The disturbed slug flow shown in this figure was a special case of the slug flow during which the lengths of bubbles of both gas and slurry as well as their frequencies changed remarkably.

The flow structures being formed were observed for various flow rates of the liquid and gas phase, different properties of the liquid phase and three pipe diameters. Very good agreement between visual observations and flow structures determined by the optoelectronic sensors was obtained.

In the investigations of multi-phase mixtures 5% water solutions of carboxymethylcellulose (CMC) and suspensions of 2–17.8wt.% spherical glass particles in CMC solutions were used as a continuous phase. A disperse species were spherical glass particles of diameters ranging from 70 to 150 μm, with the fraction of particles 90 μm in diameter being the biggest.

Suspensions of glass particles in non-Newtonian liquid solutions were treated as homogenous systems. Samples taken during the measurements confirmed with good accuracy the homogeneity of slurries used in the experiments. Further in this study, in the case of glass particles flow in CMC solutions and gas, the flow was assumed to be the two-phase non-Newtonian liquid–gas flow.

Rheological properties of CMC solutions were determined by means of Bohlin rotary rheometer model 2CV (Bohlin, England) and Rheotec RC 20 (Haake, Germany), while the rheological properties of glass particles suspension in the CMC solution were described using a

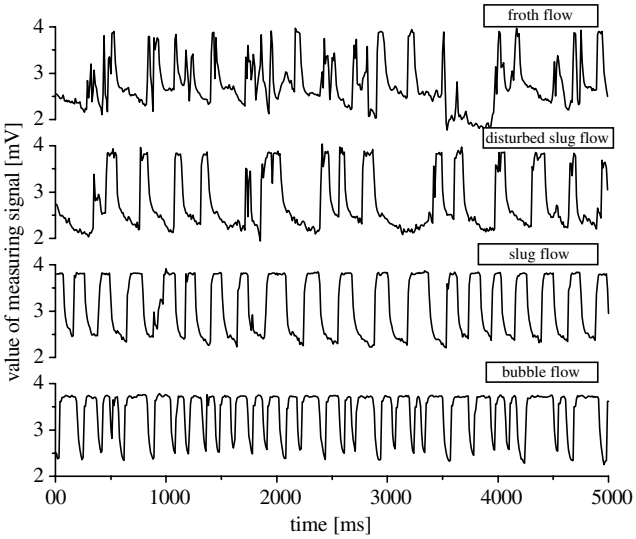

Fig. 6. "Digital oscillograms" corresponding to different flow structures.

capillary rheometer constructed by the authors and equipped with a system for mixture homogenisation (Kiljański and Fidos, 1992; Dziubiński and Fidos, 1998).

The range of rheological parameters of the tested CMC solutions and suspensions of spherical glass particles in CMC solutions—depending on the concentrations of particles and temperatures of the measurement—was as follows:

$$0.704 < n < 0.967$$

$$0.078\,\mathrm{Pa}\cdot\mathrm{s}^n < k < 1.19\,\mathrm{Pa}\cdot\mathrm{s}^n$$

3. Results and discussion

Results obtained were compared with the flow maps of two-phase Newtonian liquid–gas mixtures in vertical pipes proposed in the literature. The theoretical map of Taitel et al. (1980) and the maps proposed by Spisak (1986) and Ulbrich (1989) were analysed.

Fig. 7a–c show a comparison of the experimentally observed flow structures in vertical pipes of diameter 25.3, 40.6 and 50.5 mm with the theoretical map presented by Taitel et al. (1980).

The limits of particular flow pattern areas were determined on the basis of model equations proposed by the authors for mean parameters of the experimental media.

The point of observation of the flow patterns was the position of the optoelectronic sensor recording flow structures that occurred in the pipeline on this map. The line of transition from the slug to froth flow depends on the L_e/d ratio, where L_e is the length of the input segment of the multi-phase mixture. The value of this ratio is calculated from the model relation given by Taitel et al. (1980).

$$\frac{L_e}{d} = 40.6\left(\frac{v_M}{\sqrt{gd}} + 0.22\right) \tag{1}$$

For the experiments, the values of L_e/d ratio determined for the pipe diameters d equal 25.3, 40.6 and 50.5 mm are 83, 52 and 42, respectively.

As follows from Fig. 7a–c, the theoretical map of Taitel et al. (1980), originally developed and experimentally verified for the flow of two-phase water-air mixtures, does not describe satisfactorily our experimental data. This refers to the bubble and slug flow. The authors gave an additional criterion of the bubble flow. It has the form

$$\left(\frac{\rho_L^2 \cdot d^2 \cdot g}{\sigma_L \cdot (\rho_L - \rho_G)}\right)^{1/4} \leqslant 4.36 \tag{2}$$

This criterion was used in the investigations carried out in the pipelines 25.3 and 40.6 mm in diameter and it did not confirm the occurrence of bubble flow. So, in Fig. 7a and b the line of transition from the bubble to slug flow has not been drawn. In the case of the pipe 50.5 mm in diameter, this criterion is not satisfied and a model line separating the bubble and slug flow regions on the map can be determined—cf. Fig. 7c.

The reasons of discrepancies between the theoretical map of Taitel et al. (1980) and our experimental data can be as follows:

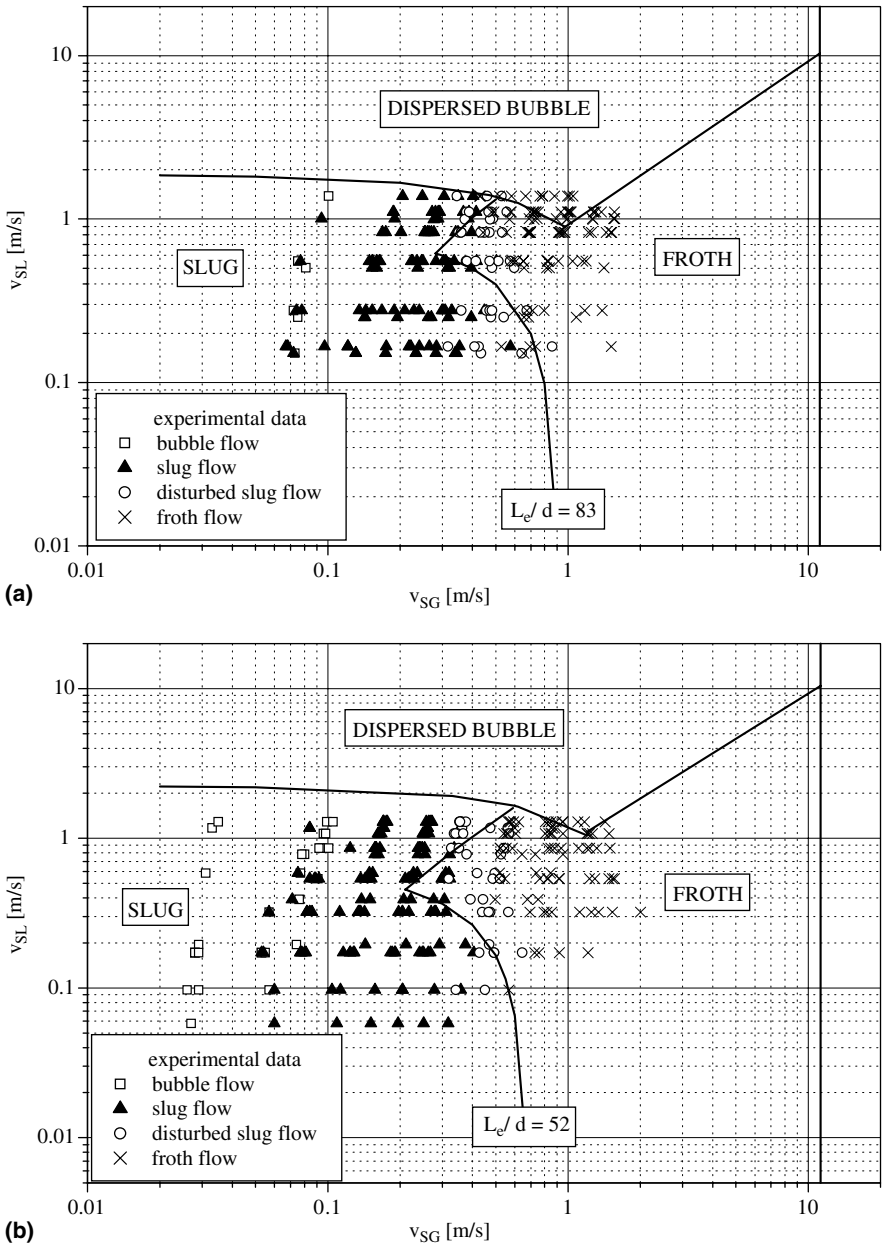

Fig. 7. Comparison of the Taitel et al. (1980) with experimental results obtained (a) in the pipeline 25.3 mm ID, (b) in the pipeline 40.6 mm ID, (c) in the pipeline 50.5 mm ID.

(a) Differences in the properties of Newtonian liquid–gas mixtures for which the model was developed and the flow of multi-phase mixtures of glass particles suspended in the non-Newtonian liquid–gas mixture used in our investigations.

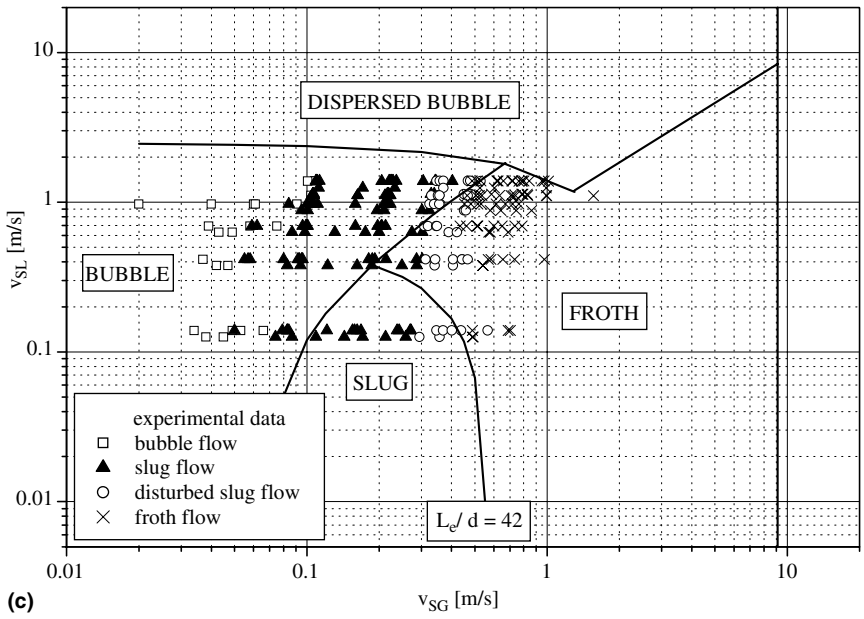

Fig. 7. (*continued*)

(b) Model assumptions taken by the authors, while constructing the map. They assumed that the transition from bubble to slug flow took place at the gas phase contribution equal to 0.25. In our experiments it occurred for much lower contribution of the gas phase in the mixture, reaching about 0.18.

The universal map of Ulbrich (1989) fails completely when used for the flow of two-phase non-Newtonian liquid–gas mixtures, cf. Fig. 8. Most experimental data that refer to bubble, slug and froth flow, are in the slug flow region on the map. This is probably not the type of liquid but the range of its viscosity that had the main impact on the lack of agreement between the experimental data and this map. Ulbrich's map was developed on the basis of a very extensive range of the author's investigations and the data published in the literature. The viscosity of all liquids flowing through the two-phase mixtures in the data bank did not exceed 46 mPa·s. Viscosities of non-Newtonian liquids used in our experiments were much higher.

Fig. 9 shows a comparison of our experimental data with generalised Spisak's map (1986). This generalisation consisted in a slight displacement of the boundary lines, separating particular flow patterns on original Spisak's map. In the original study, the author presented only a graphic form of the map. The boundary lines of the proposed generalised map that separated the ranges of different flow patterns, can be easily described by equations given in Table 2. The area concerning a disturbed slug flow can be easily distinguished on this map. The broken line represents a boundary between the slug and disturbed slug flow.

Very good agreement of the proposed map with experimental data, reaching about 92%, was obtained, although the map was prepared on the basis of the map for the two-phase flow of Newtonian liquid of viscosity exceeding 100 mPa·s—cf. Fig. 9.

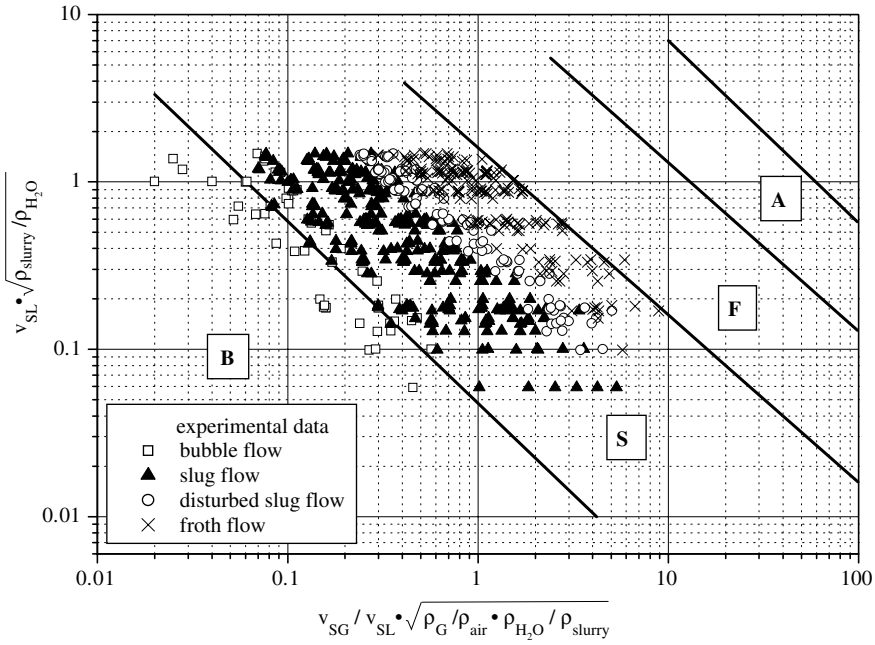

Fig. 8. Comparison of the flow patterns observed in investigations with Ulbrich's map (1989). Notation of flow pattern as in Fig. 1.

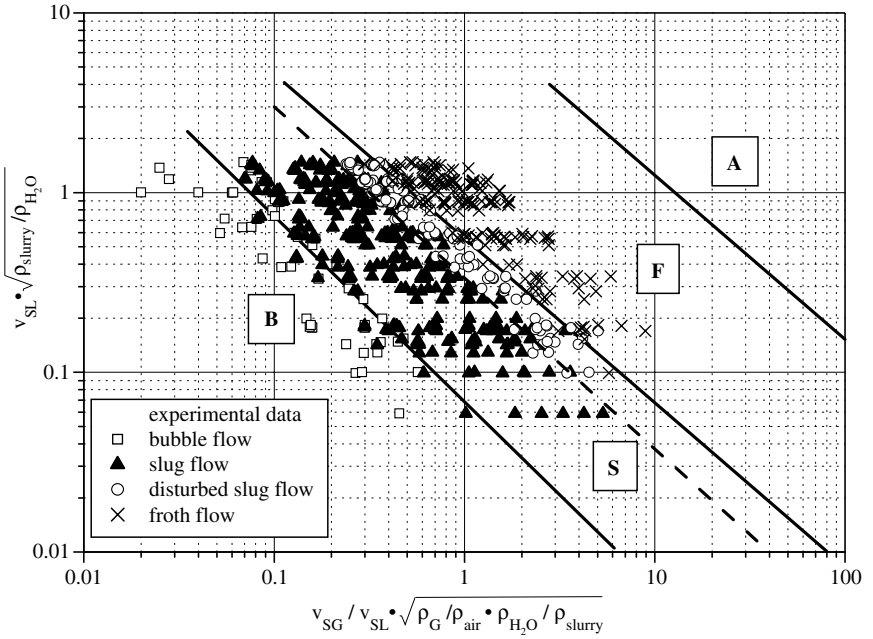

Fig. 9. Comparison of the flow patterns observed in investigations with Spisak's map (1986). Notation of flow pattern as in Fig. 1.

Table 2
Equations describing boundary lines of modified Spisak's map

Boundary between regions	Equation
Bubble–Slug (B–S)	$y = 0.0685 \cdot x^{-1.03}$
Slug–Disturbed Slug (S–DS)	$y = 0.335 \cdot x^{-0.95}$
Disturbed Slug–Froth (DS–F)	$y = 0.556 \cdot x^{-0.92}$
Froth–Annular (F–A)	$y = 10.25 \cdot x^{-0.91}$

$x = \frac{v_{SG}}{v_{SL}} \cdot \sqrt{\frac{\rho_G}{\rho_{air}} \cdot \frac{\rho_{H_2O}}{\rho_L}}$, $y = v_{SL} \cdot \sqrt{\frac{\rho_L}{\rho_{H_2O}}}$.

It is known that in the case of non-Newtonian liquid, its viscosity depends on the shear rate. An exact definition of the shear rate is possible only in the simplest flow geometries (a pipe, the space between coaxial cylinders, the space between the cone and plate) and in the case of one-phase flow only.

For the flow of a two-phase system, at a stochastic flow of bubbles in the non-Newtonian liquid, it is infeasible to define the real shear rate in the liquid, i.e. real viscosity of the liquid and viscosity of the two-phase system.

To assess viscosity of a non-Newtonian liquid in two-phase flow and to compare its range with the viscosity of a Newtonian liquid used in Spisak's map we used the effective viscosity calculated from Eq. (3)

$$\mu_{eff} = k \cdot \left(\frac{8 \cdot v_{SL}}{d} \right)^{n-1} \tag{3}$$

Such calculated values of the effective viscosity were used in several works concerning the two-phase flow of gas and non-Newtonian liquids, among others Farooqi and Richardson (1982), Heywood (1976) and Farooqi (1981).

The range of effective viscosity in the performed investigations was as presented in Table 3. Hence, all liquids used in the tests had effective viscosity higher than 100 mPa·s which corresponds to the conditions of Spisak's map (1986).

The results presented above confirm the general principle that flow rates of the liquid and gas phases have a decisive effect on the flow structure being formed (Mandhane et al., 1974; Weisman et al., 1979; Troniewski and Ulbrich, 1984; Dziubinski, 1992). Liquid viscosity starts to affect greatly the type of flow structure only for the viscosity that exceeds 100 mPa·s. This has been confirmed by many authors (Mandhane et al., 1974; Weisman et al., 1979; Govier and Aziz, 1982; Dziubinski, 1992; Fidos, 2001).

Table 3
Effective viscosity of tested experimental media

μ_{eff} [mPa·s]		
$d = 25.3$ mm	$d = 40.6$ mm	$d = 50.5$ mm
103–436	124–452	138–394

4. Conclusions

1. During the flow of multi-phase mixtures with non-Newtonian liquids, the same flow structures are observed as in the case of two-phase Newtonian liquid–gas flow.
2. In the experiments carried out for solid particle concentrations lower than 17.8wt.%, these particles had no significant effect on the type of flow being formed.
3. The applicability of generalised Spisak's map (1986) for the three-phase flow of non-Newtonian liquid–gas–solid particles was fully confirmed for the case when effective liquid viscosity was higher than 100 mPa·s.
4. It was found that non-Newtonian features of liquids had a negligible effect on the type of the two-phase flow structure. The most important appeared to be the apparent velocities of liquid and gas flow. Similar observations were made for the flow of two-phase mixtures of non-Newtonian liquid–gas in horizontal pipes (Dziubinski, 1992).

Acknowledgements

The authors wish to gratefully acknowledge the financial support provided by the Polish State Committee for Scientific Research (KBN) within grant No. 4 TO9C 024 22.

References

Barnea, D., Shoham, O., Taitel, Y., 1982. Flow pattern transition for vertical downward two phase flow. Chem. Eng. Sci. 37, 741–744.

Chhabra, R.P., Richardson, J.F., 1984. Prediction of flow patterns for cocurrent flow of gas and non-Newtonian liquid in horizontal pipes. Can. J. Chem. Eng. 62, 449–454.

Crawford, T., Weisman, J., 1984. Two-phase pattern transitions in ducts of noncircular cross-section and under adiabatic condition. Int. J. Multiphase Flow 10, 385–391.

Delhaye, J.M., 1976. Measurement techniques for studies of two-phase gas–liquid flow. Two-phase Flows Heat Transfer, Proc. Nato Adv. Study Inst. 1, 37–58.

Dziubinski, M., 1986. Flow pattern map for two-phase flow of gas and non-Newtonian fluid in horizontal pipes. Inz. Chem. Proc. 1, 3–19.

Dziubinski, M., 1992. Two-phase mixture non-Newtonian liquid–gas flow dynamic in horizontal pipes. D.Sc.thesis, Lodz Technical University, Poland.

Dziubiński, M., Fidos, H., 1998. New construction of the capillary rheometer for the rapidly sedimenting slurries. In: Proceedings of XVIth National Conference of Chemical and Process Engineering, Cracow (Vol. IV), pp. 38–41.

Farooqi, S.I., 1981. The effect of rheological properties on the flow of gas–liquid mixtures. Ph.D. thesis, University College of Swansea, Wales.

Farooqi, S.I., Richardson, J.F., 1982. Horizontal flow of air and liquid (Newtonian and non-Newtonian) in a smooth pipe, Part I. Trans. Inst. Chem. Eng. 60, 292–305.

Fidos, H., 2001. Flow hydrodynamics of multiphase mixtures of non-Newtonian liquid–gas–solid particles invertical pipes. Ph D. thesis, Lodz Technical University, Poland.

Golan, L.P., Stenning, A.H., 1969–1970. Two-phase vertical flow maps. Proc. Inst. Chem. Engrs. 184, Pt-3.

Govier, G.W., Aziz, K., 1982. The Flow of Complex Mixtures in Pipes. Van Nostrand Reinholds Co., New York.

Govier, G.W., Radford, B.A., Dun, J.S.C., 1957. The upwards vertical flow of air–water mixtures—effect ofair and water rates on flow pattern, holdup and pressure gradient. Can. J. Chem. Eng. 35, 58–70.

Griffith, P., Wallis, G.B., 1961. Two-phase slug flow. Trans. ASME. J. Heat Transfer 83, 307–320.

Hewitt, G.F., Roberts, D.N., 1969a. Investigation of interfacial phenomena in annular two-phase flow by means of the axial view technique. Report AERE-R 6070, Harwell.

Hewitt, G.F., Roberts, D.N., 1969b. Studies of two-phase flow patterns by simultaneous X-ray and flash photography, Report AERE-M 2159, Harwell.

Heywood, N.I., 1976. Air injection into suspensions flowing in horizontal pipeline. Ph.D. thesis, University of Wales, Wales.

Ikeda, T., Kotani, K., Maeda, Y., Kohno, H., 1983. Preliminary study on application of X-ray CT scanner to measurement of void fractions in steady-state two-phase flow. J. Nucl. Sci. Technol. 20, 1–12.

Kiljański, T., Fidos, H., 1992. A capillary rheometer for fast-settling suspensions. Inż. i Ap. Chem. (2), 30–31.

Lee, Y.J., Kim, J.H., 1986. A review of holography applications in multiphase flow visualization. Trans. ASME, J. Fluid Eng. 108, 279–288.

Mandhane, J.M., Gregory, G.A., Aziz, K., 1974. A flow pattern map for gas-liquid flow in horizontal pipes. Int. J. Multiphase Flow 1, 537–553.

McQuillan, K.W., Whalley, B.P., Hewitt, G.F., 1985. Flooding in vertical two-phase flow. Int. J. Multiphase Flow 11, 741–760.

Nicklin, D.J., Davidson, J.F., 1962. The onset of instability in two-phase slug flow. Symposium in Two-Phase Fluid Flow, London.

Oshinowo, T., Charles, M.E., 1974. Vertical two-phase flow. Flow pattern correlations. Can. J. Chem. Eng. 52, 25–35.

Spedding, P.L., Ngyuen, V.T., 1980. Regime maps for air–water two-phase flow. Chem. Eng. Sci. 35, 779–793.

Spisak, W., 1986. Two-phase flow of gas-highly viscous liquid. Ph.D. thesis, Wroclaw Technical University, Poland.

Taitel, Y., Barnea, D., Dukler, A.E., 1980. Modelling flow pattern transitions for steady upward gas–liquid flow in vertical tubes. AIChE J. 26, 345–354.

Troniewski, L., Ulbrich, R., 1984. Research Report WSI Opole, 102 Mechanics, 27, 29.

Ulbrich, R., 1986. The application of fiber optics to measurements of two-phase gas-liquid flow. Proc. of SPIE—Int. Soc. Opt. Eng. (Opt. Fibres Their Appl. 4) 670, 177–179.

Ulbrich, R., 1989. Two-phase gas–liquid flow identification. Studies and Monographs, 32, WSI Opole.

Weisman, J., Duncan, D., Gibson, J., Crawford, T.J., 1979. Effect of fluid properties and pipe diameter on two-phase flow patterns in horizontal lines. Int. J. Multiphase Flow 5, 437–462.